1 Semi-classical analysis

Josephson (1962) gave a theory of tunneling for Cooper pairs in terms of the *phase difference* between two superconductors separated by an insulating barrier. We can apply similar ideas here.

Let N_j, θ_j, $j = 1, 2$ be quantum variables satisfying the canonical relations

$$[\theta_1, \theta_2] = [N_1, N_2] = 0, \qquad [N_j, \theta_k] = i\delta_{jk}I,$$

from which it follows

$$\exp(i\theta_j)N_j \exp(-i\theta_j) = N_j + 1.$$

We now make a canonical change of variables

$$b_j^\dagger = \sqrt{N_j}\exp(-i\theta_j), \quad b_j = \exp(i\theta_j)\sqrt{N_j}.$$

In the mean-field approximation where N_j is large ($N_j + 1 \approx N_j$) the Hamiltonian becomes

$$H = \frac{k}{8}(N_1 - N_2)^2 - \frac{\mu}{2}(N_1 - N_2) - \mathcal{E}\sqrt{N_1 N_2}\cos(\theta_1 - \theta_2) \qquad (1)$$

We make a canonical change of variables

$$z = \frac{N_1 - N_2}{N}, \qquad \phi = \frac{N}{2}(\theta_1 - \theta_2)$$

$$N = N_1 + N_2, \qquad \chi = \frac{1}{2}(\theta_1 + \theta_2)$$

such that

$$[z, \phi] = iI, \quad [N, \chi] = iI.$$

Above, z represents the fractional occupation difference (or the *imbalance*) and ϕ the phase difference.

Setting $\lambda = kN/2\mathcal{E}$, $\beta = \mu/\mathcal{E}$ we may equivalently consider the Hamiltonian

$$H(z, \phi) = \frac{\mathcal{E}N}{2}\left(\frac{\lambda}{2}z^2 - \beta z - \sqrt{1 - z^2}\cos(2\phi/N)\right). \tag{2}$$

The Hamiltonian may be viewed as a generalisation of that for a simple pendulum

$$H(p_\theta, \theta) = \frac{p_\theta^2}{2ml^2} - mgl\cos(\theta).$$

The classical dynamics are given by Hamilton's equations of motion

$$\begin{aligned}
\frac{d\phi}{dt} &= \frac{\partial H}{\partial z} = \frac{\mathcal{E}N}{2}\left(\lambda z - \beta + \frac{z}{\sqrt{1-z^2}}\cos(2\phi/N)\right) \\
\frac{dz}{dt} &= -\frac{\partial H}{\partial \phi} = -\mathcal{E}\left(\sqrt{1-z^2}\sin(2\phi/N)\right)
\end{aligned} \tag{3}$$

with fixed points determined by $dz/dt = d\phi/dt = 0$.

- $\phi = 0$ and z is a solution of

  $$\lambda z - \beta = -\frac{z}{\sqrt{1-z^2}} \tag{4}$$

  which has a unique real solution for $\lambda > 0$.

- $\phi = N\pi/2$ and z is a solution of

  $$\lambda z - \beta = \frac{z}{\sqrt{1-z^2}}. \tag{5}$$

  which has one, two or three real solutions for $\lambda > 0$.

NOTE: When $\beta = 0$ we have maxima at

$$z = \pm\sqrt{1 - \lambda^{-2}}$$

whenever $\lambda > 1$.

Setting $f(z) = \lambda z - \beta$ and $g(z) = z/\sqrt{1 - z^2}$, fixed point bifurcations occur when $f(z)$ is the tangent line to $g(z)$ at some value z_0. At this point we have

$$\lambda = g'(z_0) = (1 - z_0^2)^{-3/2}. \tag{6}$$

Requiring $f(z_0) = g(z_0)$ gives

$$\lambda z_0 - \beta = \frac{z_0}{\sqrt{1 - z_0^2}}. \tag{7}$$

Eliminating z_0 from (6,7) yields

$$\lambda = (1 + |\beta|^{2/3})^{3/2} \tag{8}$$

which determines the parameter space boundary.

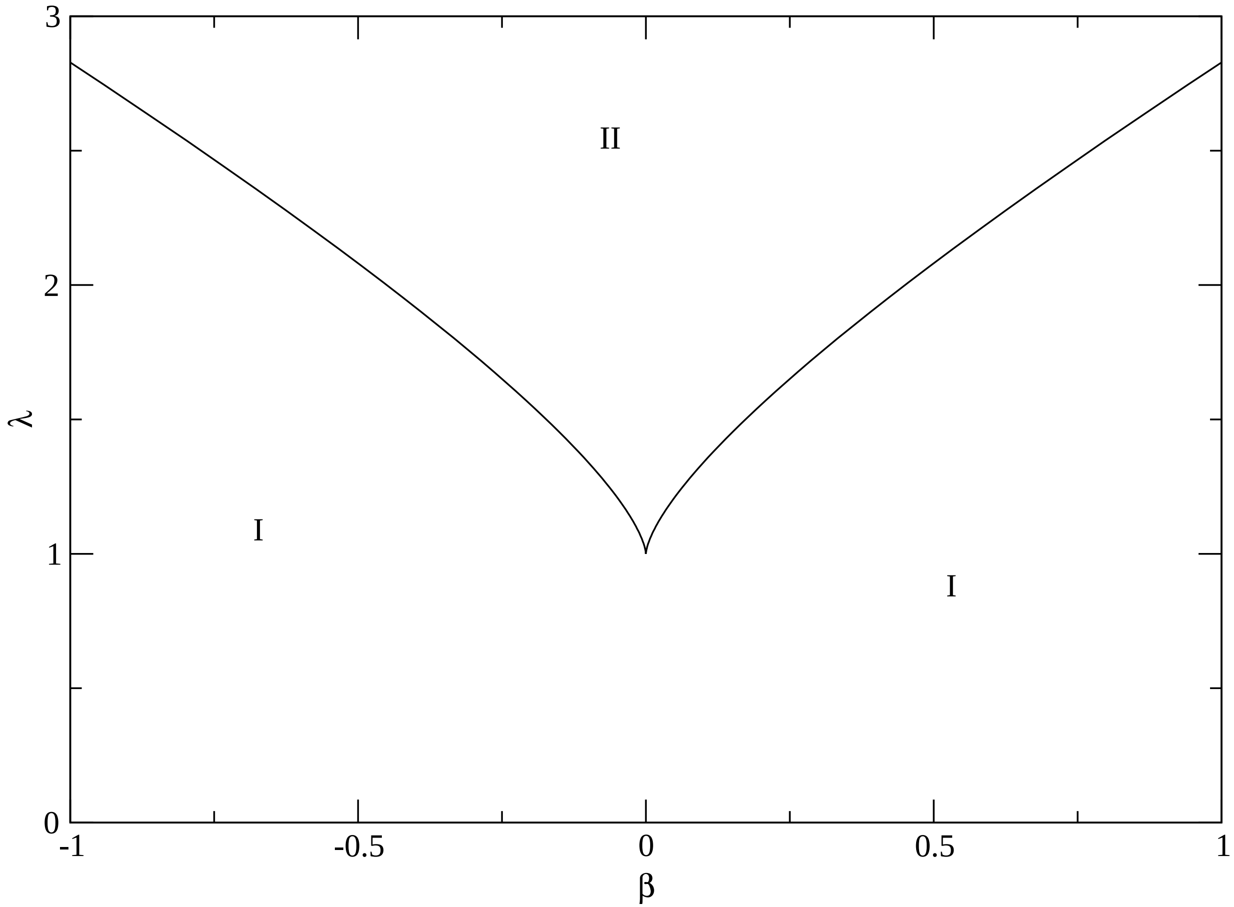

Figure 1: Coupling parameter space diagram identifying the different types of solutions for the fixed points. In region I there is just one maximum and one minimum for H. In region II there are two maxima, one minimum and a saddle point.

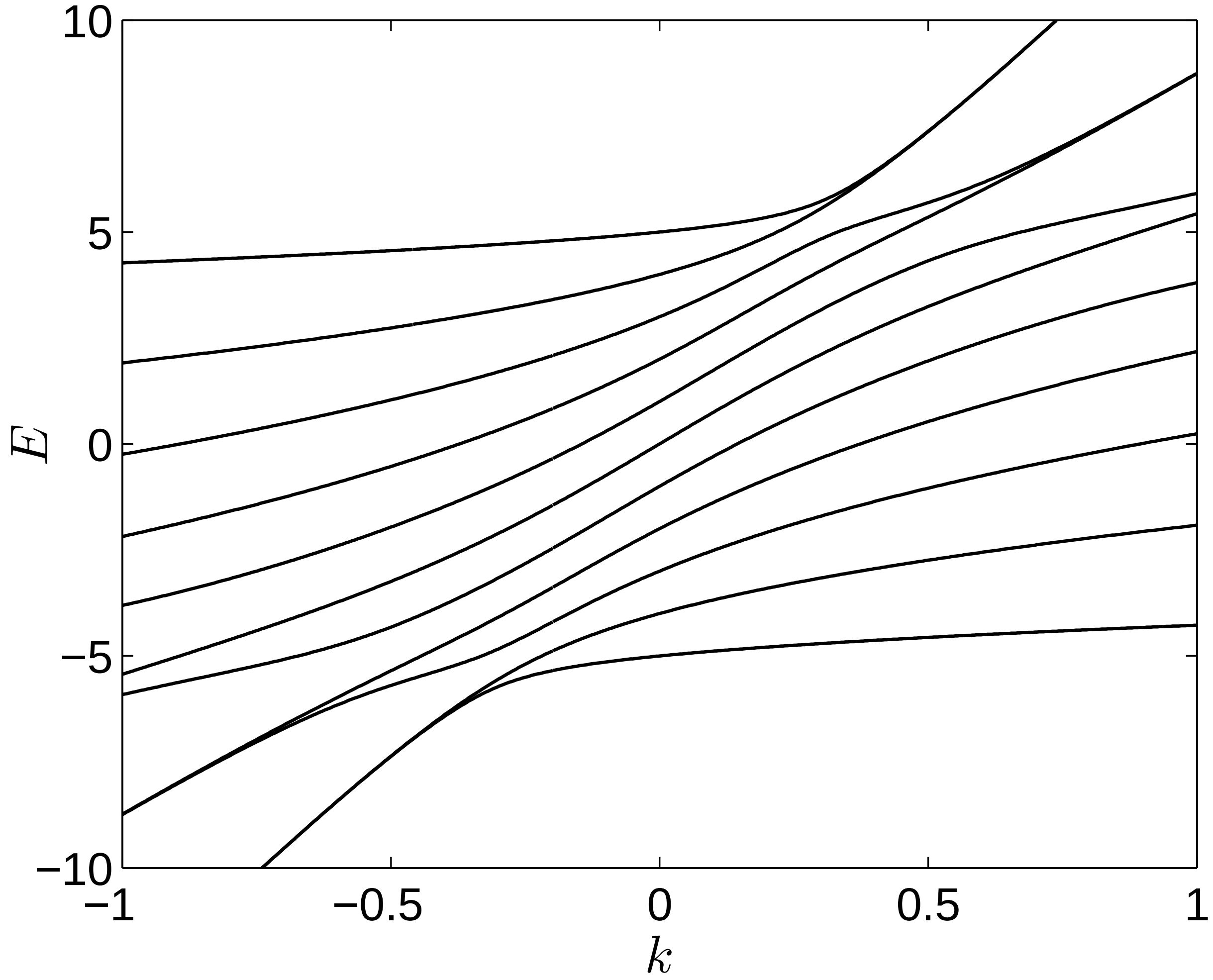

Figure 2: Energy levels versus coupling k for $N = 10$, $\mu = 0$ and $\mathcal{E} = 1$.

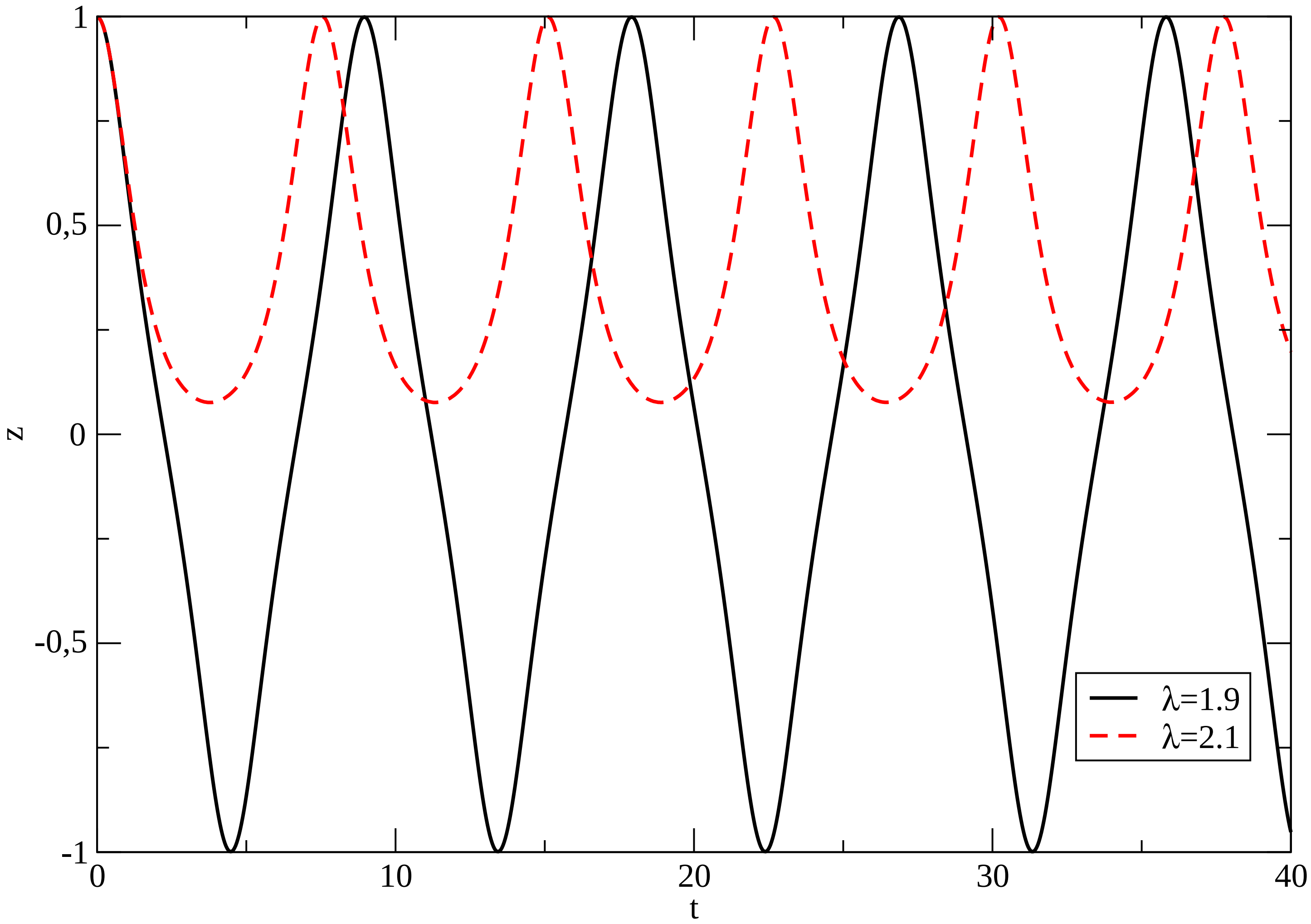

Figure 3: Time evolution for the imbalance z. The solid line is for $\lambda = 1.9$, while the dashed curve is for $\lambda = 2.1$. Other parameters are fixed at $N = 100$, $\beta = 0$, $\mathcal{E} = 1$ and the initial conditions $z(0) = 1$, $\phi(0) = 0$. The threshold coupling occurs at $\lambda_c = 2$.

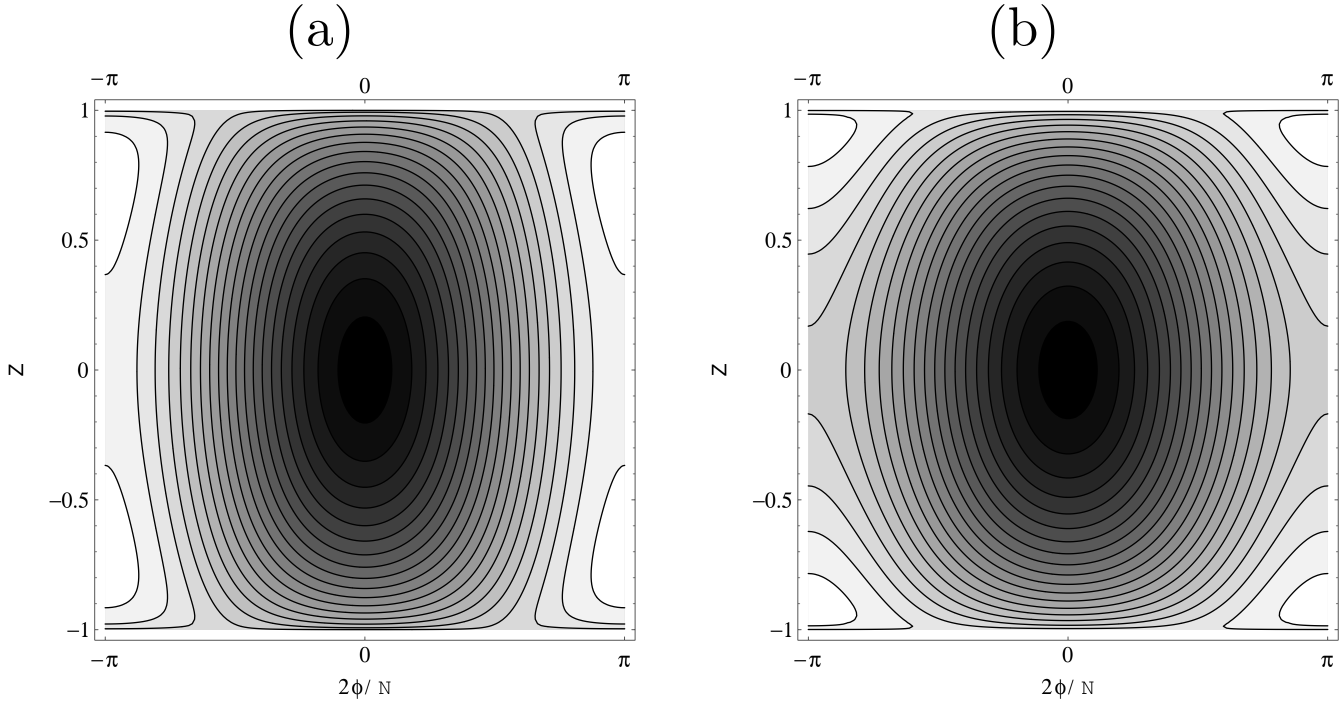

Figure 4: Level curves of the Hamiltonian (2) (a) for $\lambda = 1.5$ (below the threshold point $\lambda = 2$) and (b) for $\lambda = 2.5$ (above the threshold point $\lambda = 2$). We are using $N = 100$, $\beta = 0$ and $\mathcal{E} = 1$. Above the threshold coupling running phase modes occur leading to localised evolution of z. Below the threshold coupling the evolution of z is delocalised.

Using the initial condition $z(0) = 1$, $\phi(0) = 0$ it is found for $\beta = 0$ there is a threshold coupling $\lambda_c = 2$ separating two different behaviours in the classical dynamics, as was seen in the previous figure. The two cases may be described as

- $\lambda < 2$: Here we see that for the orbit with initial condition $z(0) = 1$, $\phi(0) = 0$, the evolution of ϕ is oscillatory and bounded in the interval $(-N\pi/2, N\pi/2)$. The evolution of z is not bounded, leading to delocalisation.

- $\lambda > 2$: Here we see that for the orbit with initial condition $z(0) = 1$, $\phi(0) = 0$, ϕ increases monotonically (running phase mode). The evolution of z is bounded in the interval $[0, 1]$, leading to localisation (self-trapping).

Recall $\lambda = kN/2\mathcal{E}$, so for fixed k and $\mathcal{E}$ we can always access the self-trapping regime by making N sufficiently large.

2 The weak tunneling limit - perturbation theory approach

To get a feel for the quantum properties here we first undertake a perturbative approach to investigate the energy gap betwen the ground state and the first excited state. Recall the Hamiltonian is

$$H = \frac{k}{8}(N_1 - N_2)^2 - \frac{\mu}{2}(N_1 - N_2) - \frac{\mathcal{E}}{2}(b_1^\dagger b_2 + b_2^\dagger b_1) \tag{9}$$

It is convenient to work in the Jordan-Schwinger spin representation

$$S^+ = b_1^\dagger b_2, \quad S^- = b_2^\dagger b_1, \quad S^z = \frac{1}{2}(N_1 - N_2)$$

such that the usual commutation relations hold.

$$[S^z, S^\pm] = \pm S^\pm, \qquad [S^+, S^-] = 2S^z.$$

This representation is $(N+1)$-dimensional when the constraint of fixed particle number $N = N_1 + N_2$ is imposed.

For simplicity, assume that $N = 2l$ is even. We define the basis states

$$|l,\, m\rangle = C_{lm}(b_1^\dagger)^{(l+m)}(b_2^\dagger)^{(l-m)}\,|0\rangle$$

with

$$C_{lm} = \frac{1}{\sqrt{(l+m)!(l-m)!}}.$$

It is found that

$$\begin{aligned}
N_1\,|l,\, m\rangle &= (l+m)\,|l,\, m\rangle \\
N_2\,|l,\, m\rangle &= (l-m)\,|l,\, m\rangle \\
b_1^\dagger b_2\,|l,\, m\rangle &= C_{lm}(b_1^\dagger)^{(l+m)}\left((b_2^\dagger)^{(l-m)}b_1^\dagger b_2 + (l-m)b_1^\dagger(b_2^\dagger)^{(l-m-1)}\right)|0\rangle \\
&= (l-m)C_{lm}(b_1^\dagger)^{(l+m+1)}(b_2^\dagger)^{(l-m-1)}\,|0\rangle \\
&= \frac{(l-m)C_{lm}}{C_{l(m+1)}}\,|l,\, m+1\rangle
\end{aligned}$$

and similarly

$$b_2^\dagger b_1\,|l,\, m\rangle = \frac{(l+m)C_{lm}}{C_{l(m-1)}}\,|l,\, m-1\rangle\,.$$

First let $\mathcal{E} = 0$, so

$$\begin{aligned} H &= \frac{k}{8}(N_1 - N_2)^2 - \frac{\mu}{2}(N_1 - N_2) \\ &= \frac{k}{2}\left(S^z\right)^2 - \mu S^z. \end{aligned}$$

Then

$$H\left|l,\, m\right\rangle = \left(\frac{k}{2}m^2 - \mu m\right)\left|l,\, m\right\rangle.$$

The states $|l,\, m\rangle$ and $|l,\, m+1\rangle$ have the same energy when

$$\mu = \frac{k}{2}(2m+1), \qquad m = 0, 1, 2, \ldots, l-1.$$

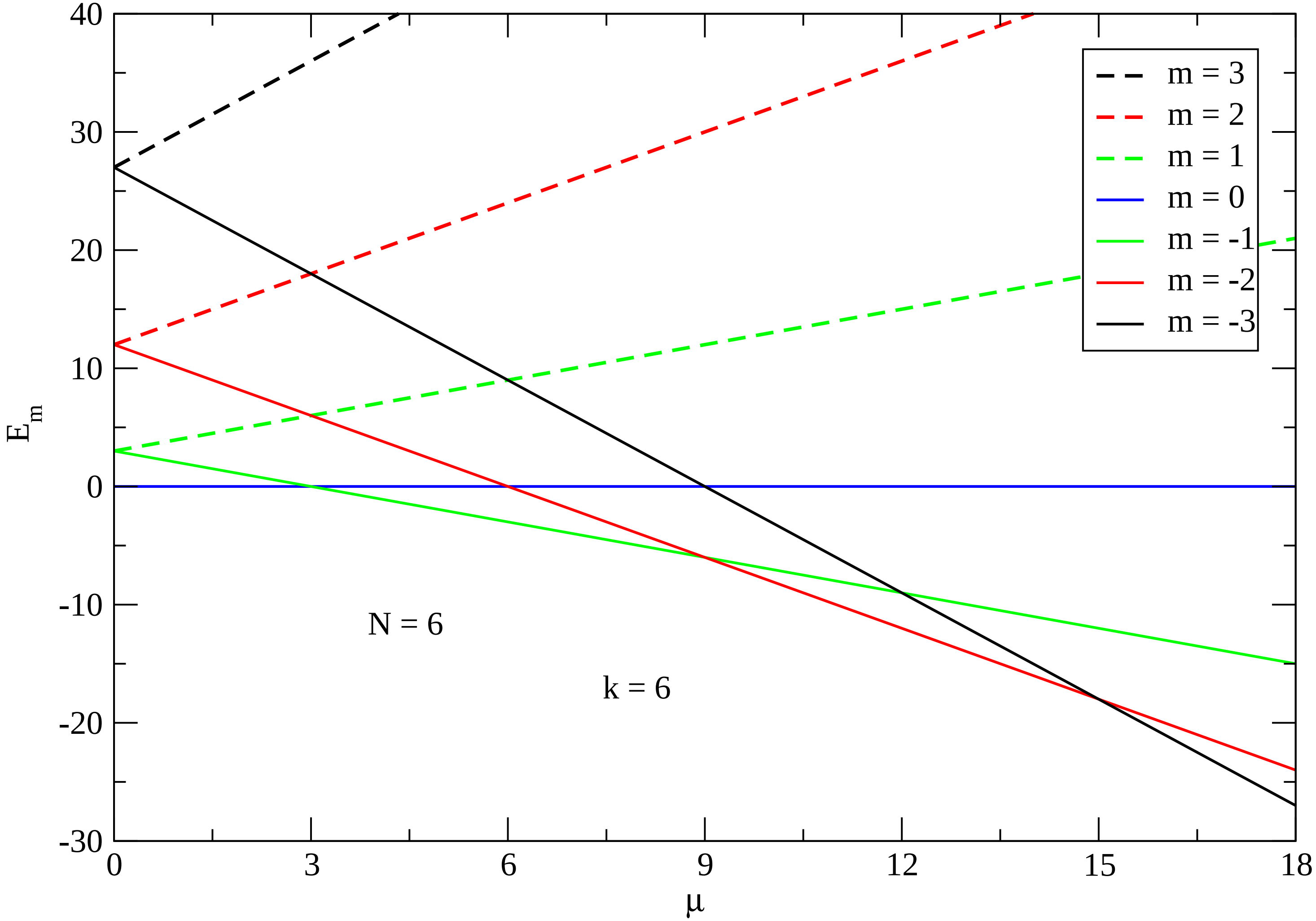

Figure 5: Energy levels versus the external potential for $\mathcal{E} = 0$, $N = 6$ and $k = 6$. The level crossings involving the lowest energy level represent changes in the ground state structure. The energy gap is also determined by level crossings involving the first excited state.

Next we define two orthogonal states, and without loss of generality we make the restriction $0 \leq \theta \leq \pi$,

$$
\begin{aligned}
|\Psi_1\rangle &= \cos(\theta)\,|l,\, m\rangle + e^{i\phi}\sin(\theta)\,|l,\, m+1\rangle \\
|\Psi_2\rangle &= \sin(\theta)\,|l,\, m\rangle - e^{i\phi}\cos(\theta)\,|l,\, m+1\rangle
\end{aligned}
$$

and weakly turn on the tunneling interaction. This gives

$$
\begin{aligned}
E_1 &= \langle\Psi_1|H|\Psi_1\rangle \\
&= \frac{km^2}{2} - m\mu + \sin^2(\theta)\left(\frac{k}{2}(2m+1) - \mu\right) \\
&\qquad - \frac{1}{2}\cos(\phi)\sin(2\theta)\mathcal{E}\sqrt{(l-m)(l+m+1)} \qquad (10)
\end{aligned}
$$

$$
\begin{aligned}
E_2 &= \langle\Psi_2|H|\Psi_2\rangle \\
&= \frac{km^2}{2} - m\mu + \cos^2(\theta)\left(\frac{k}{2}(2m+1) - \mu\right) \\
&\qquad + \frac{1}{2}\cos(\phi)\sin(2\theta)\mathcal{E}\sqrt{(l-m)(l+m+1)} \qquad (11)
\end{aligned}
$$

Now we look to minimise E_1 with respect to the variables θ and ϕ:

$$\frac{\partial E_1}{\partial \theta} = \sin(2\theta)\left(\frac{k}{2}(2m+1)-\mu\right) - \cos(\phi)\cos(2\theta)\mathcal{E}\sqrt{(l-m)(l+m+1)},$$

which is zero for

$$\cos^2(2\theta) = \frac{\left(k(2m+1)/2-\mu\right)^2}{\left(k(2m+1)/2-\mu\right)^2 + \cos^2(\phi)\mathcal{E}^2(l-m)(l+m+1)}.$$

Also

$$\frac{\partial E_1}{\partial \phi} = \frac{1}{2}\sin(\phi)\sin(2\theta)\mathcal{E}\sqrt{(l-m)(l+m+1)}$$

which is zero when $\phi = 0,\ \pi$.

The energy gap is given by

$$
\begin{aligned}
\Delta &= E_2 - E_1 \\
&= \cos(\phi)\sin(2\theta)\mathcal{E}\sqrt{(l-m)(l+m+1)} + \cos(2\theta)\left(\frac{k}{2}(2m+1) - \mu\right) \\
&= \sqrt{\left(k(2m+1)/2 - \mu\right)^2 + \cos^2(\phi)\mathcal{E}^2(l-m)(l+m+1)} \\
&= \sqrt{\left(k(2m+1)/2 - \mu\right)^2 + \mathcal{E}^2(l-m)(l+m+1)}
\end{aligned}
$$

where the last line follows since $\phi = 0,\ \pi$. It is seen that Δ is minimal when

$$
\mu = \frac{k}{2}(2m+1). \tag{12}
$$

Note that (12) is independent of $\mathcal{E}$. Thus to leading order in perturbation theory, the gap is minimal for those values of μ for which the gap vanishes when $\mathcal{E} = 0$.

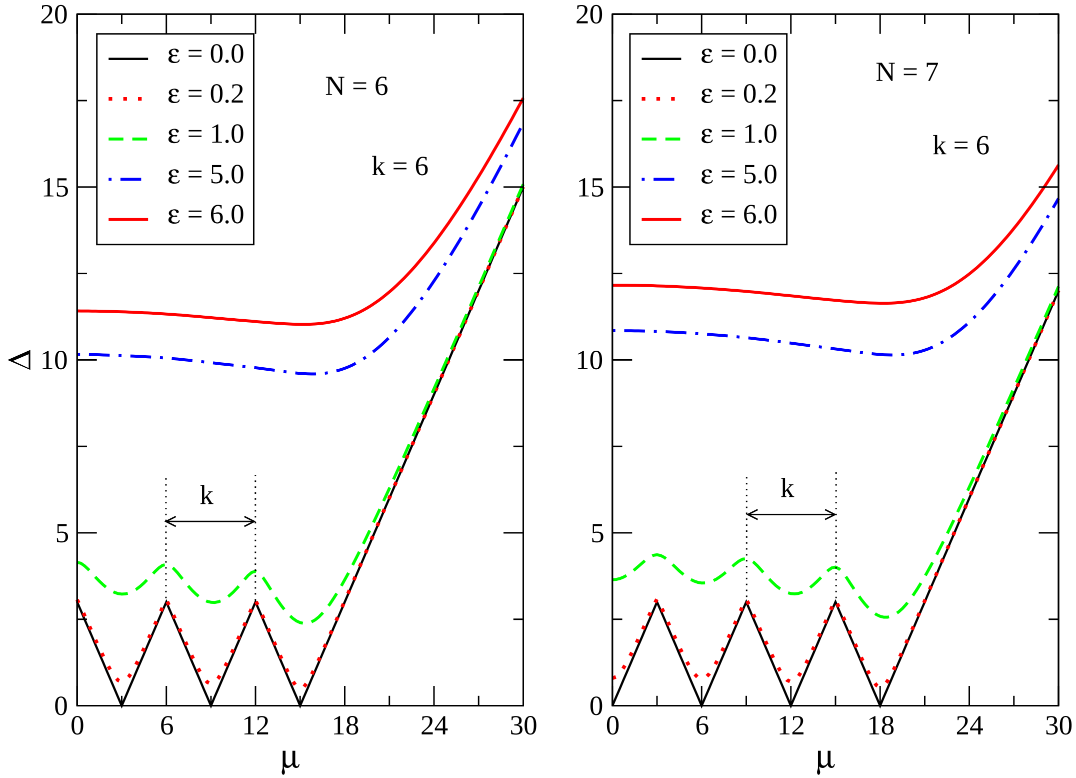

Figure 6: Energy gap Δ versus the external potential μ for different choices of the coupling parameter $\mathcal{E} = 0, 0.2, 1, 5, 6$. On the left, $N = 6$, and on the right, $N = 7$. In the extreme regime $\mathcal{E} = 0$ the minima and maxima represent the level crossings as depicted in Fig. 5. For small values of $\mathcal{E}$ the difference between two consecutive minima or maxima is constant and equal to k. As $\mathcal{E}$ increases just one minimum survives.